Received: 22 September 2020 | Revised: 21 October 2020 | Accepted: 23 October 2020
DOI: 10.37917/ijeee.16.2.7 Vol. 16| Issue 2| December 2020

Open Access

Iraqi Journal for Electrical and Electronic Engineering
Original Article

The 3-dB FBG bandwidth Characteristics

Hisham K. Hisham*
Electrical Engineering Department, Collage of Engineering, University of Basrah, Basra, Iraq

Correspondence
*Hisham K. Hisham
Electrical Engineering Department, Collage of Engineering,
University of Basrah, Basra, Iraq
Email: husham_kadhum@yahoo.com

Abstract
In this paper, the effect of the grating parameters (i.e. gratings length (L_g) and the induced index profile (Δn)); the temperature variation (T) and the applied strain change on the fiber Bragg Grating (FBG) 3dB-bandwidth (i.e. full width-half maximum (FWHM)) have successfully investigated numerically using MATHCAD software. Results show that for L_g < 7 mm, the FBG 3dB-bandwidth (i.e. full width-half maximum (FWHM)) value shows a good reliable and visible impact. Otherwise, there are no significant effects except for increasing the FBG reflectivity. Also, results show that the FWHM value has affected by the change of the Δn value. In contrast, results show that there is no significant effect of the temperature on the FWHM value. Also, results shown that the dependence of the Bragg wavelength (λ_B) upon both strain and temperature variations is lies within the range of 0.462 – 0.470 fm $\mu\varepsilon^{-1}$ °C^{-1}

KEYWORDS: FBG bandwidth, optical fiber sensor, temperature and strain sensitivity, Bragg reflectivity.

I. INTRODUCTION

The tremendous development in the fiber optic industry technology led to a huge revolution in the data transmission rate. The availability of communication links with unique features such as high reliability, fast performance, and huge ability to transmit information with a low-cost bandwidth made it a strong competitor [1, 2]. The accelerated advances in optical fiber technology have stimulated the development of optical fiber sensor technology [3]. This technology provides super advantages that do not compare with that found in the traditional sensor technology, such as the high sensitivity and variety of form factor [4, 5]. The distinctive functional characteristics of optical fiber sensors make it to the top of sensor technology and replace the well-known traditional technologies in a wide range of applications such as stress, vibration, electric fields, acceleration, pressure, temperature, humidity, viscosity and chemical measurements, etc [1, 2].

Because of their high dielectric capacity, optical fiber sensors are the best in extreme environments such as high temperatures and high pressure, as well as in environments that contain corrosive substances [6]. In addition, these sensors are fully compatible with communication systems and have the ability to perform remote sensing tasks with high efficiency [7, 8].

In recent years, optical fiber sensors-based fiber Bragg grating (FBG) have gained the largest share in the sensor market due to its many unique advantages such as small size, light weight, lack of need for electrical connections, and its ability to combat exceptional circumstances [1, 2]. These characteristics greatly contribute to showing a good performance rate with high sensitivity, accuracy, wide dynamic range and excellent efficiency [9, 10]. In addition, it is distinguished by its essential immunity to electromagnetic interference (EMI), with its rapid ability to transmit data with communication systems and widespread employment in many applications [1, 2, 11, 12].

Due to the structural and design nature of the FBG, which makes it highly sensitive to many environmental parameters, such as physical, chemical, and electrical variables, makes it used in many areas, such as space, energy, marine areas, and infrastructure [1, 12].

Physically, the FBG acts as a wavelength-dependent stop band optical filter as a result of a permanent change in the refractive index of the fiber core [6, 7, 13-21]. When the conditions for the travel mode have met, a new rejection window has appeared as a result of the constructive interference. This window is known as the Bragg window with λ_B wavelength which is totally dependent on the grating period, Λ and the effective refractive index, n_{eff} [1, 2]. As a result of this dependency, any changes in the Λ value and the n_{eff} value or in the physical model lead in a shift in the Bragg wavelength [8]. This unique behavior of the FBG parameters makes them very necessary and useful sensors tools for many important applications [1, 2]. For a uniform FBG as in Fig. 1, the Λ remain constant and the reflected light will be maximum at the λ_B value [1, 2].

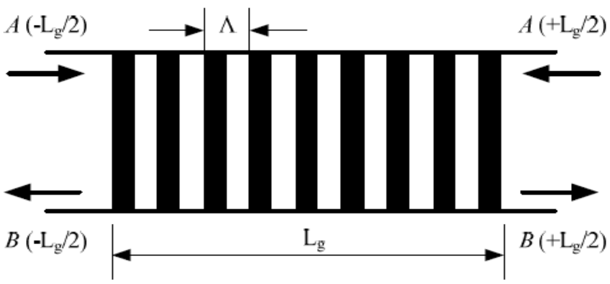

Fig. 1: Uniform fiber Bragg gratings [1, 2]

II. THEORY

Under the assumption of linear combination for the propagation modes, the electric field can give by [22]

$$E(z)=\sum_k \left\lfloor A_k^+ \exp(-j\beta_k z)+A_k^- \exp(j\beta_k z)\right\rfloor \mathrm{E}_k \quad (1)$$

In Eq. (1), A_k^+ , A_k^- , β_k and E_k are represents the amplitudes of kth mode in the +z and –z directions, the propagation constant and the modal field, respectively. According to the coupled mode theory (CMT), the electric field equations can be written as [22]

$$\frac{dA_k^+}{dz}=-j\sum_m \left\{A_m^+ C_{mk} \exp\left[-j\left(\beta_m-\beta_k\right)z\right]+ A_m^- k_{mk} \exp\left[j\left(\beta_m+\beta_k\right)z\right]\right\} \quad (2)$$

$$\frac{dA_k^-}{dz}=j\sum_m \left\{A_m^+ C_{mk} \exp\left[-j\left(\beta_m+\beta_k\right)z\right]+ A_m^- k_{mk} \exp\left[j\left(\beta_m-\beta_k\right)z\right]\right. \quad (3)$$

Based on the Fig. 1, Equations (2) and (3) are reduced to [22]

$$\frac{dA_k^+}{dz}=-j\hat{\sigma}A_k^+(z)-j\kappa^* A_k^-(z) \quad (4)$$

$$\frac{dA_k^-}{dz}=j\hat{\sigma}A_k^-(z)+j\kappa A_k^+(z) \quad (5)$$

Where $\hat{\sigma}$ and κ are the dc and ac coupling wave coefficients defined as [22]

$$\hat{\sigma}=\delta+\sigma-\frac{1}{2}\frac{d\varphi}{dz} \quad (6)$$

$$\kappa=\kappa^*=\frac{\pi}{\lambda}v\overline{\delta}n_{eff} \quad (7)$$

where $\overline{\delta n}_{eff}$ represents the dc change in the effective refractive index, ν is the fringe visibility and φ(z) is the fiber gratings chirp. In Equation 6, the factors δ and the σ are defined as [22]

$$\delta=\beta-\frac{\pi}{\Lambda}=2\pi n\left(\frac{1}{\lambda}-\frac{1}{\lambda_B}\right) \quad (8)$$

$$\sigma=\frac{2\pi}{\lambda}\overline{\delta}n_{eff} \quad (9)$$

By solving equations (4) and (5), the reflectivity of the model shown in Fig. 1 is given by [22]

$$r=\frac{\sinh^2\left(\sqrt{\kappa^2-\hat{\sigma}L_g}\right)}{\cosh^2\left(\sqrt{\kappa^2-\hat{\sigma}L_g}\right)-\frac{\hat{\sigma}^2}{\kappa^2}} \quad (10)$$

III. SENSING IN GRATING FIBER

The main elements that influence and control the FBG properties are the L_g, the Λ and the n_{eff}. In contrast, the main sensor elements in the gratings fiber are the temperature, the strain and the pressure, respectively. Therefore, the sensing mechanism works according to the amount of the wavelength shifting with a change in any of these parameters [1, 2].

A. Effect of the Temperature Change

When a change in temperature ΔT is happened, a shift in the Bragg wavelength $\Delta\lambda_B$ will be occur and can describe by [1, 2]

$$\Delta\lambda_B=\lambda_B\left(\alpha+\xi\right)\Delta T \quad (11)$$

Where,

$$\alpha=\frac{1}{\Lambda}\left(\frac{\partial\Lambda}{\partial T}\right) \quad (12)$$

$$\xi=\frac{1}{n_{eff}}\left(\frac{\partial n_{eff}}{\partial T}\right) \quad (13)$$

B. Effect of the Strain Change

By changing the applied longitudinal strain $\Delta_{\varepsilon z}$, the shifting in the λ_B will be given by [1, 2]

$$\Delta\lambda_B=\lambda_B\left(1-P_e\right)\varepsilon_z \quad (14)$$

Where P_e represent the effective strain-optic constant defined by [1, 2]

$$P_e=\frac{n^2_{eff}}{2}\left[P_{12}-v\left(P_{11}+P_{12}\right)\right] \quad (15)$$

Where P_{11}, P_{12} and υ are the fiber optic strain components and the Poisson's ratio, respectively [1, 2].

C. Effect of the Pressure Change

By changing the applied pressure, the shifting in the λ_B is obtained by [1, 2]

$$\Delta\lambda_B = \lambda_B\left[-\frac{(1-2v)}{E} + \frac{n^2{}_{eff}}{2E}(1-2v)(2P_{12}+P_{11})\right]\Delta P \qquad (16)$$

Where E represent the FBG Young's modulus.

IV. Results And Discussion

In this paper, our analysis based on a uniform FBG single-mode silica fiber with 1550 nm as shown in Fig. 1 and the all typical values used in the simulation are in Ref. [1, 2, 6, 7, 19].

Figure 2 show the effect of grating length (L_g) on the FBG full width-half maximum (FWHM) characteristics at constant temperature (i.e. at room temperature [19]). As shown, when L_g = 1 mm, the FWHM spectra is about 1.6 nm and reduced to the 1.52 nm by increasing the L_g to the 2 mm. More increasing in the L_g value to the 3 mm leads to reduce the 3-dB spectra to the 1.4 nm and has reduced to the 1.28 nm by increasing the L_g value to the 5 mm. However, this behavior of decreasing the FBG FWHM with the increasing of the L_g value does not continue, where for $L_g > 7$ the is no significant effect on the 3-dB spectra and is maintained approximately at 1.0 nm for more increasing in the L_g value until 10 mm. Conversely, the FBG reflectivity has significantly affected by the L_g value. Where, it has increased approximately from 58% to the 98 % with the increasing of the L_g from 1mm to 10mm as shown in Fig.3.

Figure 4 show the effect of temperature (T) on the grating reflectivity for L_g = 10 mm. In this analysis, T has varied from 10 ^oC to T_o + 10 ^oC (i.e. T_o is assumed as a reference temperature (i.e. T_o = 25 ^oC) [1, 6, 7, 8, 19]). Results shown, a shift in the λ_B by a rate of a 0.12 nm/^oC has happened due the strong temperature grating refractive index dependence [1, 2, 6, 7, 8, 19]. This shifting affected significantly on the peak reflected value. In contrast, there is no significant or clear effect on the FWHM spectra as shown in Fig. 5 and in Fig. 6. This behavior is due to the fact that the change in the temperature resulting in a total shift in the reflectivity spectrum with constant distance between the first two zeros (i.e. FWHM [1, 2]), thereby; the total spectrum do not change.

Fig. 8 shows the effect of fiber refractive index change (Δn) on the FBG FWHM characteristics for L_g = 10 mm. It's clearly that the FWHM increases with the increase of the Δn value and this increment significantly increases by increasing is approximately linear especially for Δn = 0.4 x 10^{-4}.

Figure 9 show the effect of strain variation on the λ_B. Results shown that the λ_B has increasing linearly with the strain change and with a rate of 1.2 pm/με. This increasing in the λ_B with the increase of the applied stress will affect the system; especially at high stress values, where the shift in the wavelength may exceed more than 2 nm. Therefore, the stress must be controlled in order any improper case.

Finally, Fig. 10 shows the effect of both the strain and the temperature variations on the Bragg wavelength. Results show a clear correlation between the change in both temperature and stress on the shift value of Bragg wavelength, and this effect may be increase significantly for a large temperatures or stress ranges.

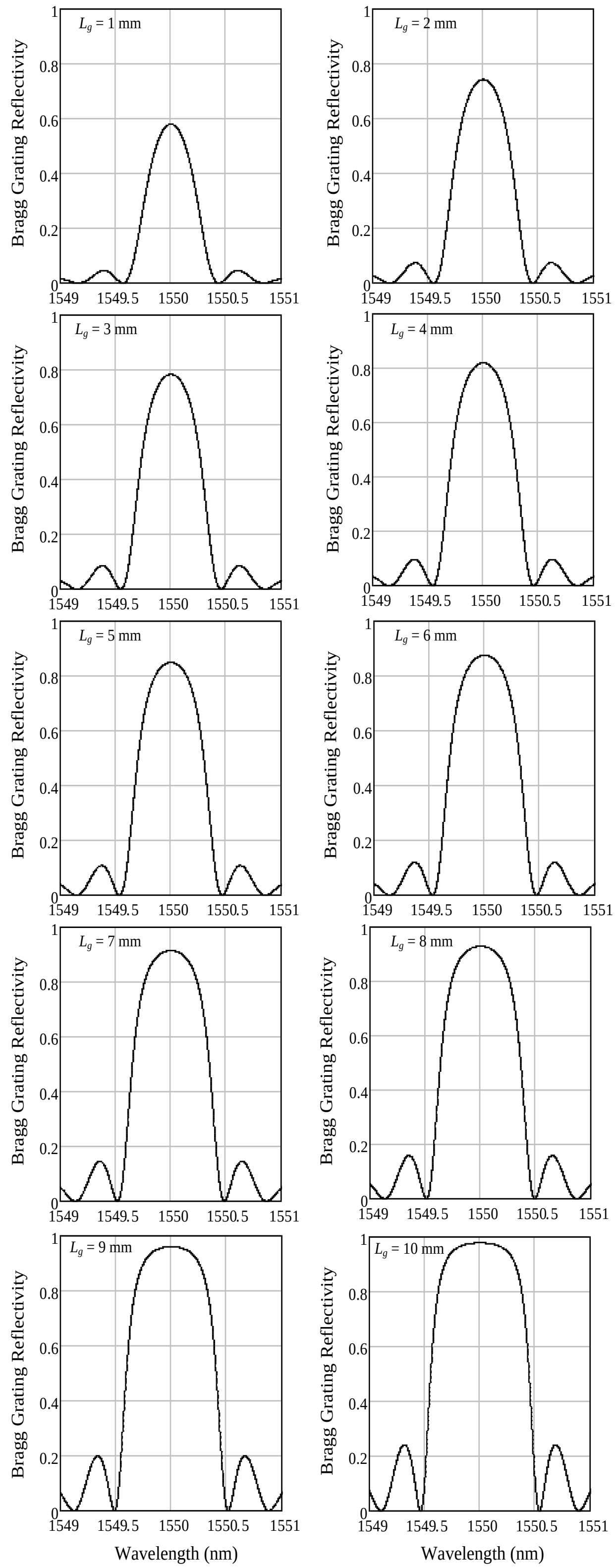

Fig. 2: Effect of grating length (L_g) on the 3-dB spectra.

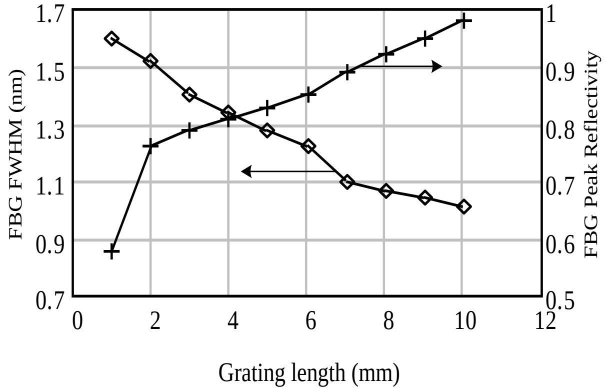

Fig. 3: Effect of grating length (L_g) on both the FBG 3-dB and the peak reflectivity.

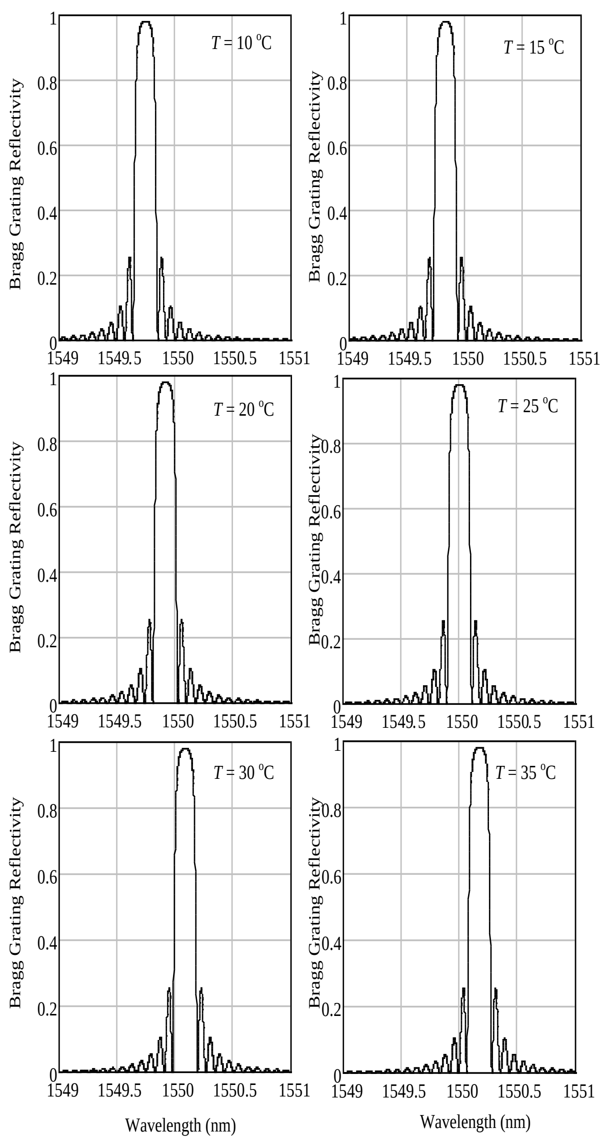

Fig. 4: Effect of temperature on the grating reflectivity.

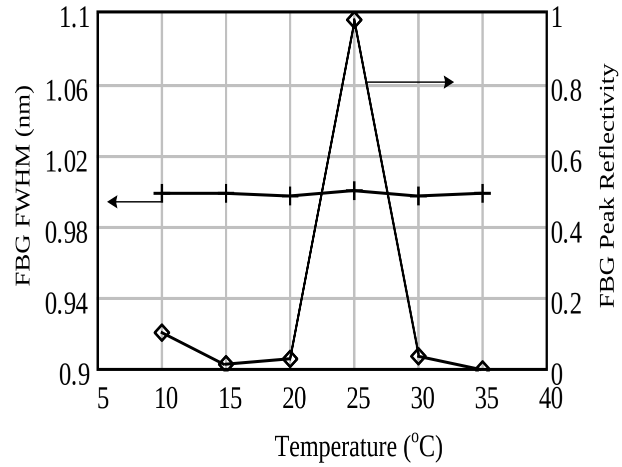

Fig. 5: Temperature effect on both the 3-dB spectra and the peak reflectivity.

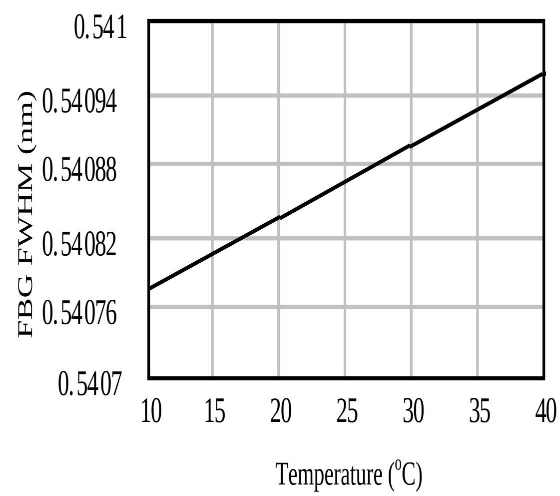

Fig. 6: Effect of temperature on the 3-dB spectra.

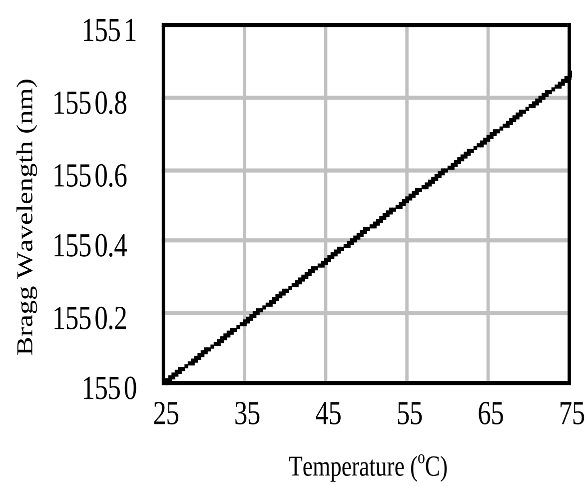

Fig.7: Bragg wavelength vs temperature variation

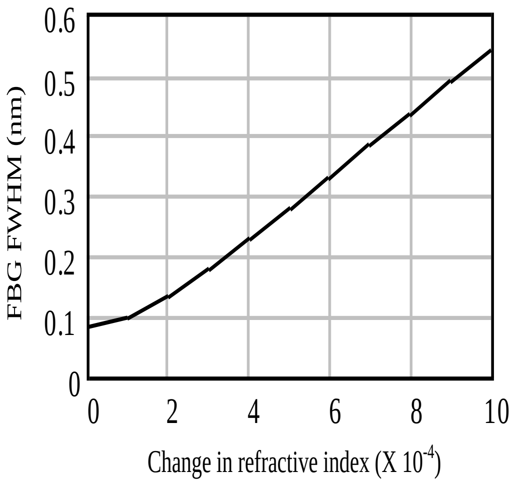

Fig. 8: Effect of *Δn* on the 3-dB spectra.

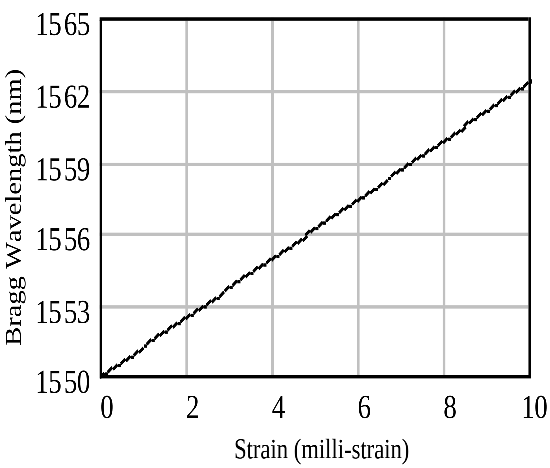

Figure 9: Effect of strain on Bragg wavelength.

V. Conclusions

The effects of the grating length (L_g), the fiber refractive index change (Δn), the temperature (T) variation and the applied strain change are investigated numerically on the FBG as a sensor model using MATHCAD software successfully. It is found that the FWHM can be increasing by optimizing the L_g value and with the increase of the Δn value. Thus, for a strong FBG with large FWHM characteristics to be achieved, the L_g with 6 mm has to be sufficient and the Δn must be as large as possible. Also, results show that by changing temperature 50 °C, the tuning value in the λ_B not excited 1 nm. Also, results shown that the dependence of the λ_B upon the strain and the temperature variations is lies within the range of 0.462 – 0.470 fm $\mu\varepsilon^{-1}$ °C^{-1}.In contrast, there is no significant effect on temperature variation on the FBG 3-dB value.

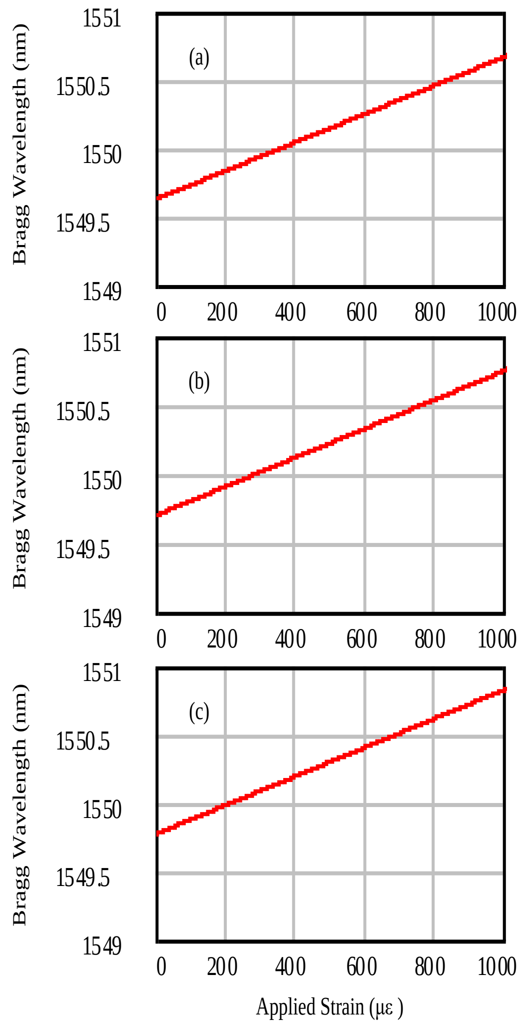

Fig. 10: Effect of temperature on strain response.

Conflict of Interest

The authors have no conflict of relevant interest to this article.

References

[1] Hisham K. Hisham, Fiber Bragg Grating Sensors: Development and Applications, CRC Taylor & Frances, 1st edition, June 2019.

[2] A. Othonos, and K. Kalli, Fiber Bragg Gratings: fundamentals and applications in telecommunications and sensing, Artech House, Norwood, 1999.

[3] P. G. E. Lumens, "Fibre-optic sensing for application in oil and gas wells", P.hD thesis, Eindhoven University of Technology, 2014.

[4] A. C. Gringarten, T. von Schroeter, T. Rolfsvaag, and J. Bruner, "Use of Downhole Permanent Pressure Gauge Data to Diagnose Production Problems in a North Sea Horizontal Well," SPE Conference, 2003.

[5] T. Unneland, "Permanent Downhole Gauges Used in Reservoir Management of Complex North Sea Oil Fields," SPE, 1994.

[6] Hisham K. Hisham, “Numerical Analysis of Thermal Dependence of the Spectral Response of Polymer Optical Fiber Bragg Gratings”, Iraq J. Electrical and Electronic Engineering, Vol.12, pp.85-95, 2016.

[7] Hisham K. Hisham, “Effect of Temperature Variations on Strain Response of Polymer Bragg Grating Optical Fibers”, Iraq J. Electrical and Electronic Engineering, vol. 1, pp.53-58, 2017.

[8] H. K. Hisham, “Theory of Dispersion Reduction in Plastic Optical Gratings Fiber”, J. Opt. Commun., V. 9, pp.2-4, 2018.

[9] A. M. B. Braga, "Optical Fiber Sensors for the Oil and Gas Industry," in Advanced Photonics, Optical Society of America, 2014.

[10] C. E. Campanella, A. Cuccovillo, C. Campanella, A. Yurt and V. M. N. Passaro, “Fibre Bragg Grating Based Strain Sensors: Review of Technology and Applications”, Sensors, V. 18, pp. 31-51, 2018.

[11] G. Allwood, G. Wild and S. Hinckley, “Fiber Bragg Grating Sensors for Mainstream Industrial Processes”, Electronics, V. 6, pp. 83-92, 2017.

[12] Hisham K. Hisham, “Full width-half maximum characterstics of FBG for petroleum applications”, Iraq J. Electrical and Electronic Engineering, vol. 16, pp.99-103, 2020.

[13] Hisham K. Hisham, “Turn_On Time Reduction in VCSELs by optimizing laser parameters”, Iraq J. Electrical and Electronic Engineering, vol. 12, pp.146-154, 2016.

[14] J. Dorleus, Y. Zhang, J. Ning, T. Koscica, H. Li, and H. L. Cui, “A Fiber Optic Seismic Sensor for Unattended Ground Sensing Applications”, ITEA Journal, V. 30, pp. 455–460, 2009.

[15] L. F. Mennella, M. Esposito, A. Cusano, M. Giordano, G. Breglio, S. Sorge, C. C. Tassini, A. Torre, G. D’Altrui, A. Cutolo, “A Fiber Optic Bragg Grating Seismic Sensor”, IEEE Photonics Technology Letters, V. 19, pp. 1991 – 1993, 2008.

[16] J. Wang, T. Liui, G. Song, H. Xie, L. Li, X. Deng, and Z. Gong, “Fiber Bragg Grating (FBG) Sensors Used in Coal Mines”, PHOTONIC SENSORS, V. 4, pp. 120–124, 2014.

[17]Y. Zhang, S. Li, J. Ning, Z. Yin and H–L Cui, “Seismic wave detection system based on fiber optic sensor”, Proc. SPIE. Earth Observing Systems, September 2006.

[18] Y. R. Garc, J. M. Corres, and J. Goicoechea, “Vibration Detection Using Optical Fiber Sensors”, Journal of Sensors, V. 12, pp. 11-55, 2010.

[19] Hisham K. Hisham, “Bandwidth Characteristics of FBG Sensors for Oil and Gas Applications”, American Journal of Sensor Technol., V. 4, pp. 30-34, 2017.

[20] D. J. M. Snelders and A. Boersma, “Development of thermo-stable FBG optical sensor for oil and gas applications”, Proc. of the 8th Inter. Conf. on Sensing Technolo., pp. 278-281, 2014, UK.

[21] K. T. V. Grattan and T. Sun, “Fiber optic sensor technology: an overview,” Sensors and Actuators A: Physical, vol. 82, pp. 40-61, 2000.

[22] G. P. Agrawal and N. K. Dutta, Semiconductor Lasers, 2nd ed. (New York: van Nostrand Reinhold, 1993).